CHAPTER 5

SIMULATION RESULTS ANALYSIS

5.1 Introduction

This chapter presents the comparative analysis/studies based on the simulation findings in chapter 4. Chapter 4 shows that three important data sets can be created for underwater acoustic data transmission and how they can be used to determine the optimal data packet size qualified by two performance metrics – throughput efficiency and energy efficiency (with implicit EPUB element) for different BERs. These qualifiers are collectively defined by the author as "the two performance metric qualifiers" or in short as "*2Q*". It is important to highlight here that the entries in the three data sets can be represented by three different graphs as shown respectively in Figure 4.6, Figure 4.7, and Figure 4.10 in chapter 4.

It is apparent from the proposed algorithm and the relevant graphs that the computed packet size eventually is a compromise between optimal packet length (size) obtained based on throughput efficiency and energy efficiency. It is well understood that energy is always one of the main issues in underwater wireless sensor network (in fact in terrestrial wireless sensor network too) because the power source in the sensor nodes is very often non-rechargeable and at times non-replaceable. Therefore the analysis/studies discussed in this chapter are taking energy efficiency as the basis for comparison. That is, the optimal packet size obtained under different performance metrics or the combination of the metrics is compared in the context of energy efficiency. The analysis/studies in this chapter will comprise of:-

(i) Comparing the optimal data packet size (ODPS) based on BER only with the ODPS produced by the proposed algorithm in the context of energy efficiency.

(ii) Comparing the ODPS qualified by throughput efficiency (in terms of lR product) as the only performance metric qualifier with the ODPS produced by the proposed algorithm in the context of energy efficiency, and

(iii) Comparison of the ODPS based on both BER and throughput efficiency as the performance metrics qualifiers with the ODPS produced by the proposed algorithm in the context of energy efficiency.

In terrestrial radio wave communications certain WSN data transmission has been shown in [55] (for a single hop transmission) and [56] (multi-hop transmission) that CSMA protocol in the MAC layer could help to improve the performance of pure Aloha protocol. Readers are reminded here that the works in this research were based on Aloha protocol at the MAC layer. Therefore the author would like to leave a direction of research for those interested readers to extend the analysis/studies in this chapter to include the analysis between the proposed algorithm under CSMA protocol (instead of Aloha protocol) in UWASN in a single hop context. Single hop is highlighted here because the proposed algorithm is meant only for data transmission between a source-sink pair. Multi-hop environment could be left, again, as another research direction for the interested readers.

5.2 Result Analysis

5.2.1 Optimal Data Packet Size Based on BER against Proposed Algorithm

The main objective of the analysis in this subsection is to investigate how the energy efficiency in the selected data packet size based *only* on BER differs from the energy efficiency in the ODPS obtained from the proposed algorithm that uses two performance metric qualifiers (2Qs). The main reference data set in this analysis will be extracted from the database that was used to construct the basic graphs in Figure 4.6 on page 74. No doubt, for a more meaningful and comprehensive comparison, it is necessary to regenerate the data set with finer granularity. It means that a new data set needs to be generated to hold finer details of relating optimal data packet size (N_{opt}) to different BERs based on more header length. It implies that, it is necessary to have Figure 4.6 plotted with more detailed data points.

The complete N_{opt} entries for the new data set can be found in the excel file in Appendix C and are used to plot the graphs shown in Figure 5.1. It should be noticed that the new set of graphs obtained is for different header length varying from 30 bits to 100 bits with an increment of 10 bits. It is understood that a header length between 40 and 100 bits is a norm in practical data packet transmission.

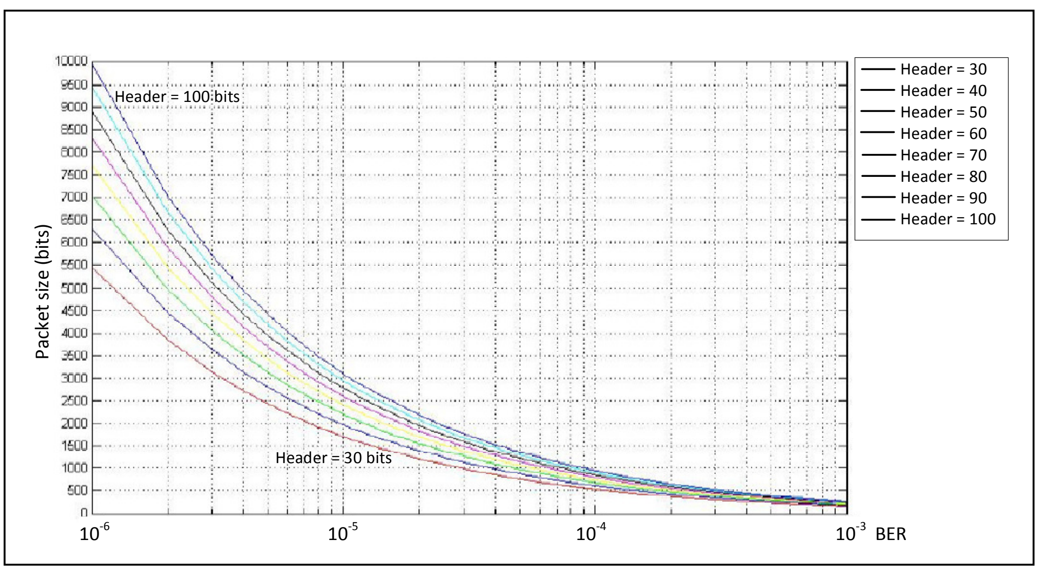

Figure 5.1: Packet size against BERs with header length from 30 bits to 100 bits.

For analysis purpose, some of the important BERs and N_{opt} under various h can be extracted from Appendix C into a simplified and more readable table format as shown in Appendix D. The table in Appendix D can be further modified into the format shown in Table 5.1 below. Full table entries for Table 5.2 can be found in Appendix E.

Table 5.1: Optimal data packet size against BERs under different header length

Header = 30		Header = 40			Header = 100	
BER	N_{opt}	BER	N_{opt}		BER	N_{opt}
10^{-1}	20	10^{-1}	20		10^{-1}	1
10^{-2}	37	10^{-2}	39		10^{-2}	36
:	:	:	:		:	:
10^{-6}	5462	10^{-6}	6304		10^{-6}	9949

Now each of the N_{opt} entries in Table 5.1 can be used as an index for indexing into the data set of Figure 4.10 on page 82 to get the respective value of energy efficiency. Keep in mind that Figure 4.10 gives various energy efficiency plots. Again, for more comprehensive studies, the basic graphs in Figure 4.10 need to be enhanced by including more BERs. The enhanced version of Figure 4.10 is plotted and shown in Figure 5.2.

As can be seen in the enhanced plot of Figure 5.2, each BER listed in Table 5.1 can be properly reflected in each of the BER lines in the figure. Take note that Figure 5.2 is for a header length of 80 bits. This plot is simply shown here as an example to illustrate the data (and the graphs) needed for the comparative studies undertaken by the author. Sets of data for energy efficiency for header length of 30 bits to 100 bits can be found in Appendix F(samples). Each of the data set covers a range of BERs from a very noisy link of $p = 10^{-2}$ to a high quality link of $p = 10^{-6}$.

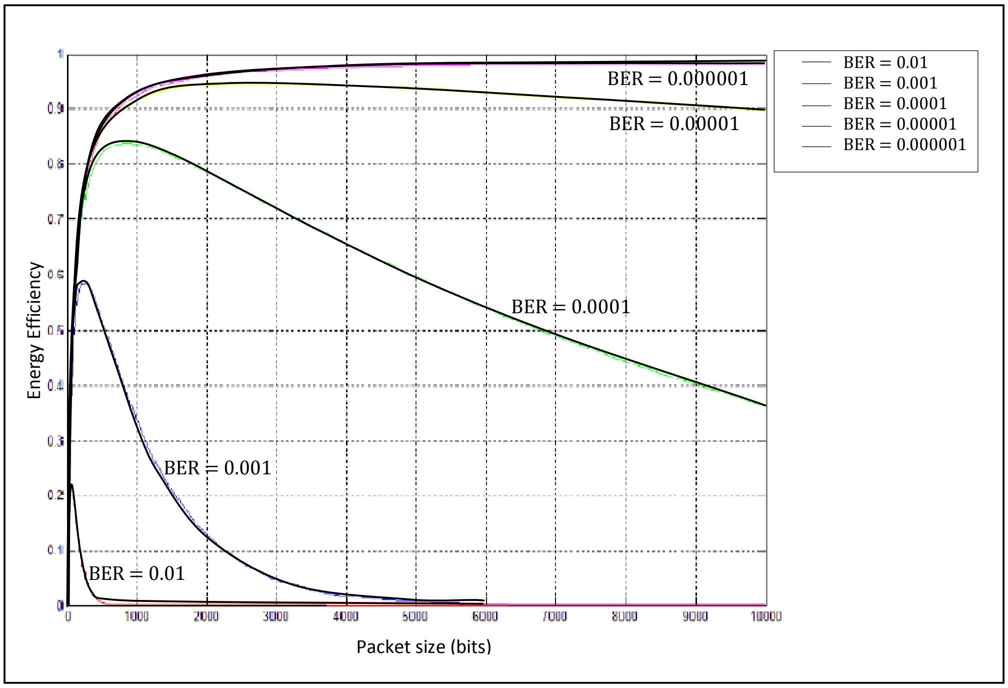

Figure 5.2: Enhanced graphs for energy efficiency against packet size under different BERs for a header length of 80 bits.

With the energy efficiency values obtained from graphs (or the data set) in Figure 5.2, Table 5.1 can then be modified to hold these values (the energy efficiency) in a column labeled as E_η adjacent to N_{opt} as shown in Table 5.2. The complete table is given in Appendix G.

Table 5.2: Optimal packet size against BERs and the related energy efficiency (E_η).

Header = 30			Header = 40				Header = 100		
BER	N_{opt}	E_η	BER	N_{opt}	E_η		BER	N_{opt}	E_η
10^{-1}	20	-	10^{-1}	20	-		10^{-1}	1	-
10^{-2}	37	0.35	10^{-2}	39	0.31	. .	10^{-2}	36	0.17
:	:	:	:	:	:		:	:	:
10^{-6}	5462	0.99	10^{-6}	6304	0.99		10^{-6}	9949	0.98

Then another column can be added adjacent to E_η in Table 5.2 to hold the energy efficiency values from the optimum packet size computed using the proposed 2Q optimization algorithm. This column is shown in Table 5.3 as E_{2Q} – literally meaning energy efficiency with 2 qualifiers. The full table entries can be found in Appendix H.

Table 5.3: Comparison of N_{opt} and E_η based on BER only against N_{2Q} and E_{2Q} based on the proposed algorithm in the context of energy efficiency with lR product of 1×10^5 m-bps.

Header = 30						Header = 100				
BER	N_{opt}	E_η	E_{2Q}	N_{2Q}		BER	N_{opt}	E_η	E_{2Q}	N_{2Q}
10^{-1}	20	-	-	-		10^{-1}	18	-	-	-
10^{-2}	37	0.35	0.34	59		10^{-2}	41	0.27	0.18	76
10^{-3}	157	0.71	0.68	265		10^{-3}	197	0.65	0.53	397
10^{-4}	532	0.90	0.88	934		10^{-4}	681	0.87	0.81	1,428
10^{-5}	1716	0.97	0.96	3,056		10^{-5}	2210	0.96	0.93	4,694
10^{-6}	5462	0.99	0.99	9,771		10^{-6}	7045	0.99	0.98	15,019

The entries in columns E_η and E_{2Q} are to be compared side by side. Finally column N_{2Q} is placed next to column E_{2Q} for showing the relevant optimal packet size computed from the proposed algorithm. It should be pointed out here that the E_{2Q} entries in Appendix H are based on a *range-rate* (lR) product of 1×10^5 m-bps. This lR value may be taken as equivalent to a range/distance of 10 meters between a source node and a sink node communicating with a data rate of 10kbps. Two more tables were created using the identical format of Table 5.3 for different lR products are shown in Appendix I and Appendix J.

The BERs, N_{opt}, E_n, E_{2Q}, and N_{2Q} in Table 5.3 can now be used to plot the graphs in Figure 5.3 for analysis purpose. Take note that due to a large variation in packet sizes, from tens of bits to thousands of bits, a log scale is adopted for plotting the N_{opt} and N_{2Q} values. For the BERs, its axis is also labeled in a log scale with an increment step of a decade, and for the energy efficiency its scale is normalized into a scale ranging from 0 to a maximum of 1.

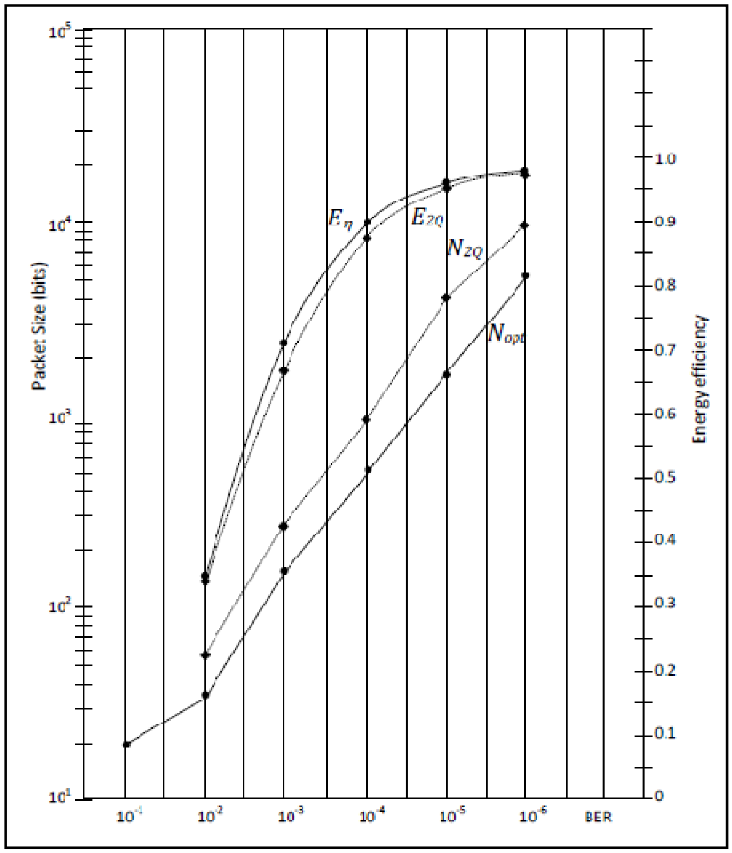

Figure 5.3: Comparison of N_{opt} and E_η against N_{2Q} and E_{2Q} based on full table entries in Appendix H for packet header size of 30 bits.

Figure 5.3 clearly shows that the energy efficiency from the proposed algorithm is comparable to the energy efficiency based solely by BER. E_{2Q} curve is seen to be slightly below the E_η curve but upon careful analysis, their difference in the worst case is found to be less than 3% meaning that the energy efficiencies shown here are practically similar.

In terms of optimal packet size, as seen in Figure 5.3 the N_{2Q} curve is always above the N_{opt} graph suggesting that the proposed algorithm seems to be able to generate larger packet size than the approach by using BER as the sole qualifier. Further, it can be shown that, with careful analysis, on average the data packet size computed from the proposed algorithm (2Q) is about 60% larger than the packet size computed using BER as the sole qualifier. This shows that the proposed 2Q algorithm is able to generate larger data packet size with comparable energy efficiency.

For a more complete or perhaps a more meaningful comparative study, the data in Appendix I (for *IR* product of 5x10^5 m-bps), and data in Appendix J (for *IR* of 9x10^5 m-bps) are used to plot out the graphs shown in Figure 5.4 and Figure 5.5.

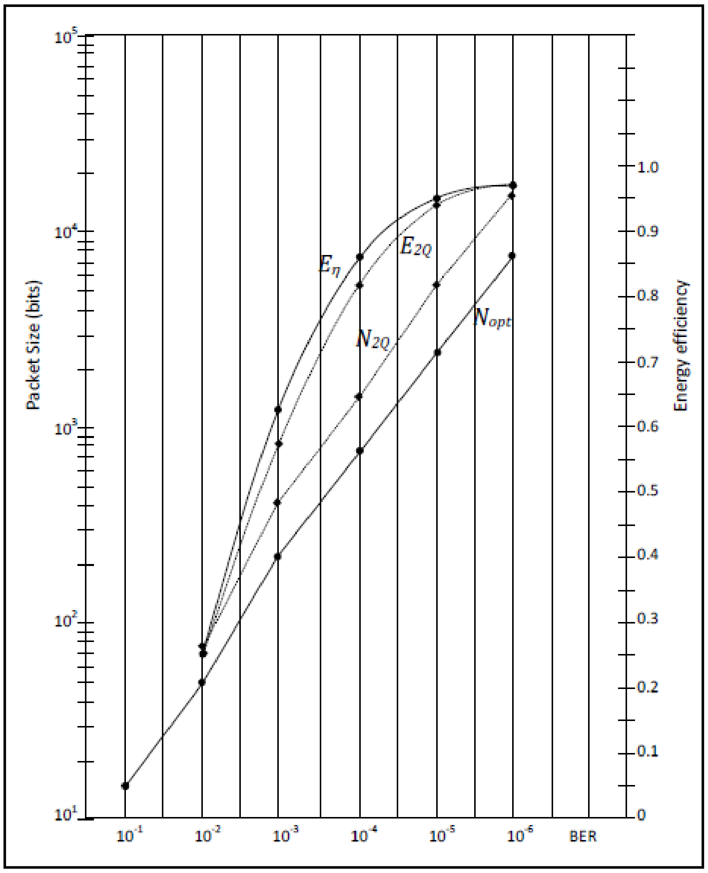

Figure 5.4: Comparison of N_{opt} and E_η against N_{2Q} and E_{2Q} based on full table entries in Appendix I for packet header size of 60 bits.

The *IR* values in Appendix I and Appendix J respectively indicate a range of 50m and 90m between the source-sink nodes transferring data at the rate of 10kbps. Notice also that the headers of different sizes were chosen to plot Figure 5.3 to 5.5. These header values were picked in such a way that they somehow covered the headers ranging from 30 bits to 100 bits. The graphs corresponding to the entries in Appendix I and Appendix J are consecutively shown below.

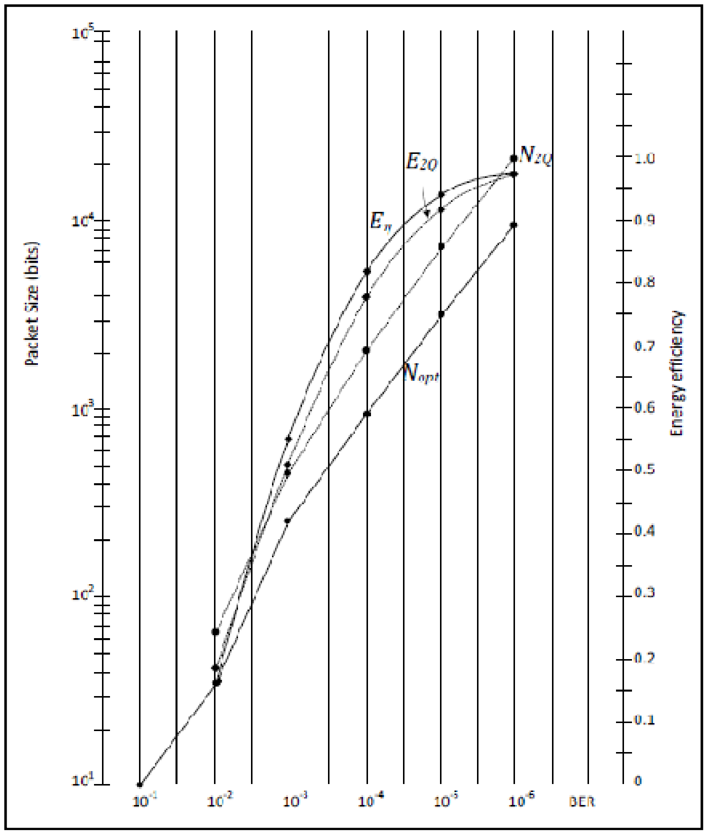

Figure 5.5: Comparison of N_{opt} and E_η against N_{2Q} and E_{2Q} based on full table entries in Appendix J for packet header size of 100 bits.

With different packet header length and *IR* products, Figure 5.4 and Figure 5.5 show a similar graph pattern to that in Figure 5.3. Both figures indicate that E_{2Q} is comparable to E_η , meanwhile N_{2Q} is better than N_{opt}.

Another point of interest from the above three graphs is that N_{2Q} is getting significantly larger than N_{opt} and yet maintaining a reasonably fair energy efficiency as the link quality is getting better i.e. approaching smaller BER (or *p*). This may suggest that the proposed 2Q algorithm can better optimize data packet size than the single qualifier approach when the UW link quality is good. However it is important to remind that 2Q may need a little more computation time than 1Q.

5.2.2 Optimal Data Packet Size Qualified by Throughput Efficiency against Proposed Algorithm

The objective of this comparative study is to investigate how the energy efficiency in the selected data packet size based on throughput efficiency as the *only* qualifier differs from the energy efficiency for the packets based on the proposed 2Q algorithm. The main reference data set in this study will be extracted from the database used to construct the basic graphs in Figure 4.7 on page 77. Again, as in the analysis study in 5.2.1 above, the graphs in Figure 4.7 is enhanced with more p (or Pe or BER) granularities to reflect and relate the BERs used in Table 5.3. This is necessary to ensure that the analysis are consistent in the context of energy efficiency.

The enhanced plot of Figure 4.7 is shown in Figure 5.6. It needs to consider that this plot is for a header length of 80 bits to make it consistent within the header length of 30 bits to 100 bits. A whole set of data for optimal data packet size against different lR products (realizing that lR product contains throughput efficiency information) for header length of 30 bits to 100 bits can be found in Appendix K.

Figure 5.6 can now be used to construct a table with various entries as shown in Table 5.4 which are fully shown in Appendix L. This table is so constructed for having the similar format as that in Table 5.1 where N_{opt} is the optimal packet size for various lR products under different p (the link quality). The readers should recall that lR and p are related to throughput efficiency. Therefore these two elements are used in constructing Table 5.4.

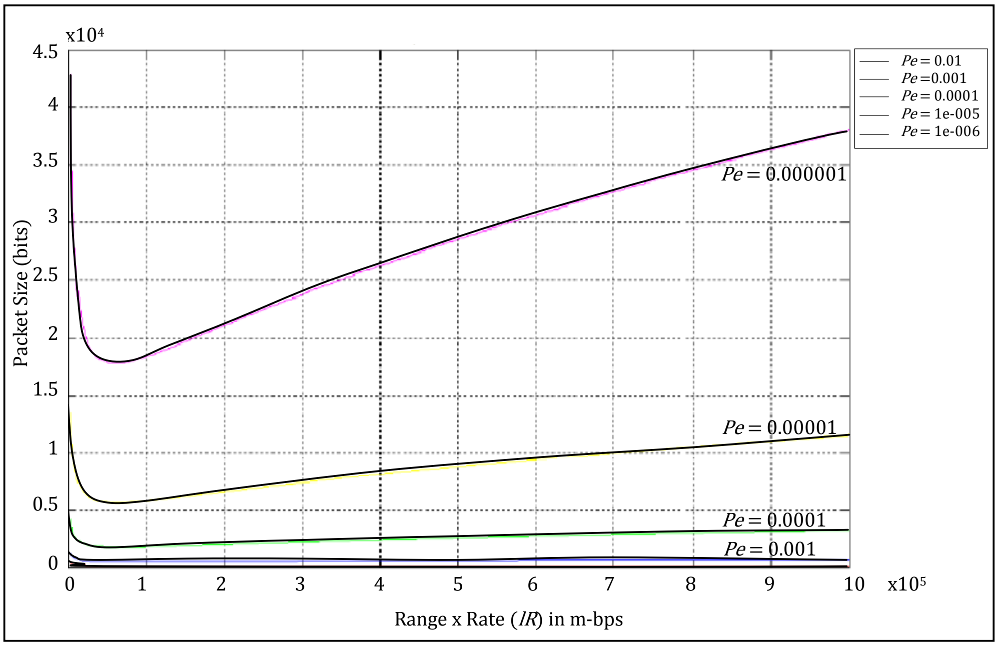

Figure 5.6: Enhanced plot of optimal data packet size against *lR* products under different P_e granularities for a packet header length of 80 bits

Table 5.4 is constructed for a header length of 80 bits. It then needs to note that for each different header length there will be a table similar to Table 5.5 associated to it. In other words, with an increment of 10 bits for header length from a range of 30 to 100 bits, there would be a total of 8 such tables.

Table 5.4: Optimal packet size against *lR* product under different *p* for a header length of 80 bits.

$p = 10^{-2}$		$p = 10^{-3}$			$p = 10^{-6}$	
lR ($\times 10^5$)	N_{opt}	*lR* ($\times 10^5$)	N_{opt}		*lR* ($\times 10^5$)	N_{opt}
1	106	1	487		1	18,380
2	100	2	520		2	21,070
:	:	:	:		:	:
9	98	9	692		9	36,310

Now using the similar method and process as described in section 5.2.1, a table similar to the format of Table 5.2 can be constructed. It is shown in Table 5.5 below, the full entries of which can be found in Appendix M.

Table 5.5 holds the values of the optimal data packet size (N_{opt}) and the energy efficiency (E_{IR}) obtained from Figure 5.6 and Figure 5.2 respectively. The entries in columns E_{2Q} and N_{2Q} are the energy efficiency and the optimal data packet size computed from the proposed 2Q algorithm. E_{2Q} and N_{2Q} values are tabulated in Table 5.5 for direct comparison to E_{IR} and N_{opt}.

Table 5.5 Comparison of N_{opt} and E_{IR} (based on IR product) against N_{2Q} and E_{2Q} (based on proposed algorithm) in the context of energy efficiency for a header length of 80 bits.

$p = 10^{-2}$						$p = 10^{-6}$				
IR (x10^5)	N_{opt}	E_{IR}	E_{2Q}	N_{2Q}		IR (x10^5)	N_{opt}	E_{IR}	E_{2Q}	N_{2Q}
1	106	0.19	0.21	73		1	18,380	0.98	0.98	13,640
2	100	0.18	0.21	70		2	21,070	0.98	0.98	14,987
:	:	:	:	:		:	:	:	:	:
9	98	0.18	0.21	68		9	36,310	0.98	0.98	22,607

The IR products, N_{opt}, E_{IR}, E_{2Q}, and N_{2Q} from Table 5.5 in Appendix M now can be used to plot the graphs as shown in Figure 5.7 showing the relationships among packet size, IR product, and energy efficiency. With IR value started at 1x10^5 m-bps, the packet size is found to be more than a thousand bits. Therefore the packet size axis starts at 1000 instead of at 0. The energy efficiency scale is again normalized to a maximum of 1.

As following on from the preceding subsection and for a more meaningful and comprehensive comparison, two more tables with identical format to that of Table 5.5 were created for header length of 30 bits and 100 bits as shown in Appendix N and

Appendix O respectively. The data in these two tables are used to plot the graphs shown in Figure 5.8 and 5.9 for comparative studies purpose.

A glance in Figure 5.7 reveals that the N_{opt} is very much better than N_{2Q} and straightforwardly shows that N_{opt} is almost always double the N_{2Q} value. However, large packet size of N_{opt} seems to be not bringing along with it a good increase in energy efficiency.

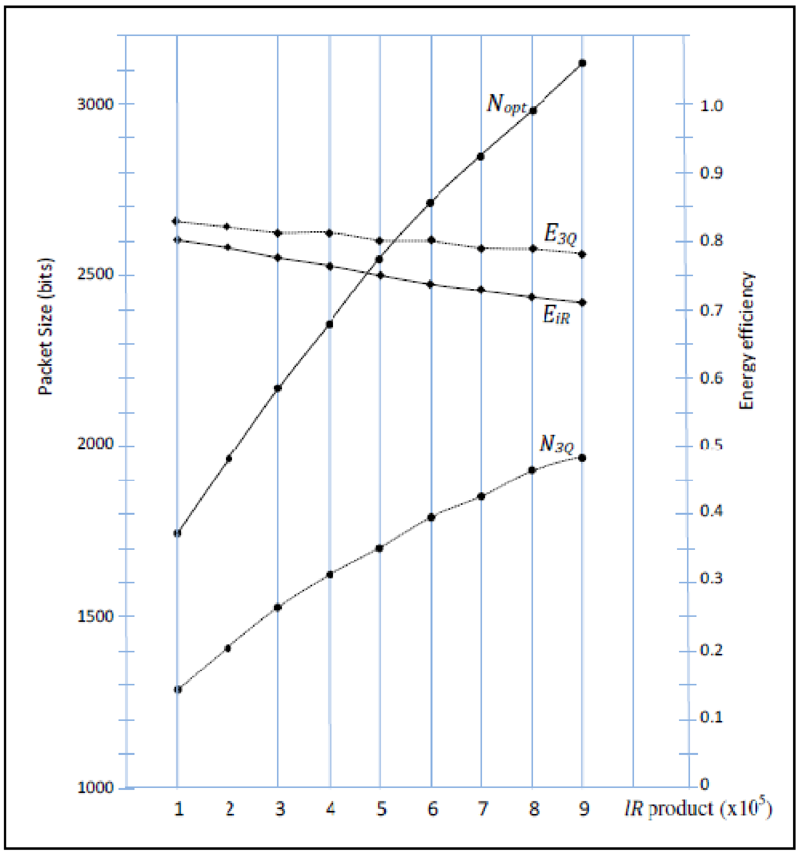

Figure 5.7: Comparison of N_{opt} and E_{IR} against N_{2Q} and E_{2Q} based on full table entries in Appendix M for header length of 80 bits with p of 10^{-4}.

Through a careful comparison, it should be noticed that the smaller N_{2Q} packet size is in fact having an energy efficacy (of E_{2Q}) much better than that in E_{IR} (energy efficiency computed based on N_{opt} value). In the event of large IR product value e.g. at $9\text{x}10^5$ m-bps, a difference of almost 10% between E_{2Q} and E_{IR} can be seen. A difference of 10% in energy efficiency could be a concerned in underwater sensor node energy conservation.

A large data packet size transmitted under large *lR* product brings along a lower energy efficiency can be explained from the fact that, with large *lR* (range-rate) value it means either the range between a source-sink pair is large or the rate of data transmission is high, of which, in either cases may result in a higher probabilities of data packet corruption/error. Hence a higher demand for data packet retransmissions, which means more energy wastage, will bring the energy efficiency down. For this, it would be wise to have a smaller packet size when *lR* is large to attain much better energy efficiency.

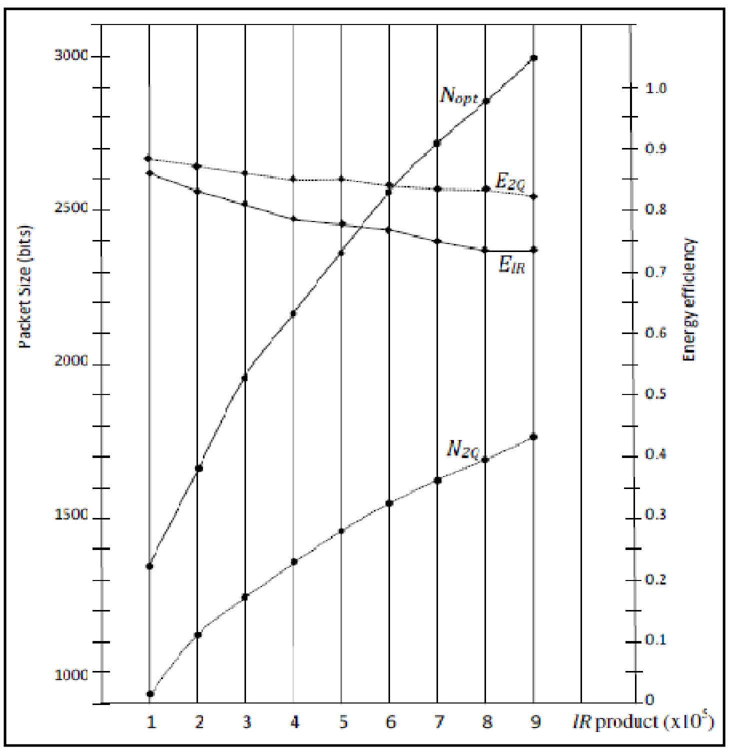

Figure 5.8: Comparison of N_{opt} and E_{lR} against N_{2Q} and E_{2Q} based on full table entries in Appendix N for header length of 30 bits with p of 10^{-4}.

The plots in Figure 5.8 and 5.9 show the equal facts as the ones in Figure 5.7. It is hereby for the author to say that the proposed 2Q algorithm with two qualifiers is able to suggest a data packet size with higher energy efficiency than the data packet size computed based on throughput efficiency (with its *IR* product) alone.

Other interesting information that can be extracted from Figure 5.7 to 5.9 is that, if data packet size of 1000 bits is taken as the base line in these graphs, N_{opt} size at *IR* value of 9x10^5 m-bps is about doubled than that of the N_{2Q}. However at this *IR* value the N_{opt} packet suffer an energy efficiency dropped by almost 10%. For this, E_{2Q} is seemed to be better than E_{IR} by almost 10%. This could be quite an issue in terms of energy conservation for underwater wireless sensor nodes if the power source for the nodes are not chargeable or replaceable.

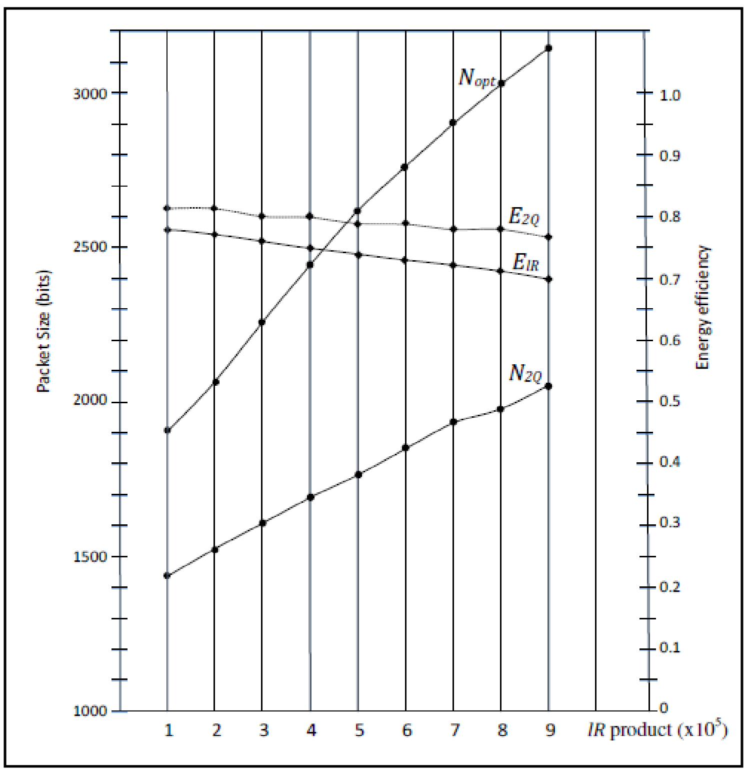

Figure 5.9: Comparison of N_{opt} and E_{IR} against N_{2Q} and E_{2Q} based on full table entries in Appendix O for header length of 100 bits with *p* of 10^{-4}.

At this juncture the author would like to point out that with a p of 10^{-4}, there is a total of 8 tables that can be created for a header length of 30 bits to 100 bits with an increment step of 10 bits. That is, of course, 8 graphs can be plotted out for comparative studies. The author plotted all the eight graphs out and intentionally found them to have similar pattern to that of Figure 5.7 to 5.9. As a result, only three of these graphs are presented here to illustrate the comparisons and the rest of the tables and their related graphs are intentionally left out in this dissertation.

The author would like to mentioned here that in fact there are more than 8 tables/graphs that can be generated based on the 5 values of p, ranging from 10^{-2} to 10^{-6}, used in the simulations described in chapter 4. With each p bringing along 8 tables (and therefore 8 graphs) a total of 40 tables and 40 graphs are then to be possible. The author shall leave all these tables and graphs to the readers for their further exploration interest.

5.2.3 Optimal Data Packet Size based on BER and Throughput Efficiency against Proposed Algorithm

This subsection describes the analysis/studies on how the energy efficiency in the selected data packet size based on both BER and throughput efficiency as the performance metrics (simply called 2M) differs from the energy efficiency of the optimal data packet size computed by the proposed 2Q algorithm. The reader may refer to the algorithm presented in section 4.3.4 on page 85 to find that this 2M approach is in fact the implementation of the proposed algorithm but stops at line 10. This is the focal point for the analysis to be described in this subsection.

A database with the format shown in Table 5.6 was created for this analysis and comparative studies. In the table, the column N_p holds the values of optimal packet size extracted from the graphs in Figure 5.1 (graphs of BERs against packet sizes) with reference a to a certain header length. The entries in the column N_{IR} are the optimal packet size extracted from Figure 5.6 (IR products against packet sizes) with reference to a certain IR product. Column labeled N_{2M} is the average of N_p and N_{IR}.

Column labeled as E_{2M} shows the energy efficiency of data packet size based on both BER and throughput efficiency i.e. the 2M approach.

Table 5.6: Optimal packet size qualified by BER and lR product and its energy efficiency compared to energy efficiency from proposed algorithm.

Header = h (bits)						
lR product = r (m-bps)						
BER	N_p	N_{lR}	N_{2M}	E_{2M}	E_{2Q}	N_{2Q}
10^{-1}						
10^{-2}						
:						
10^{-6}						

The E_{2M} value is obtained by using a related N_{2M} value as an index for the horizontal 'packet-size' axis in Figure 5.2 (plot of packet sizes against energy efficiency) whereby the corresponding E_{2M} (energy efficiency) value can be vertically looked up under the desired BER curve/graph. For instance, if N_{2M} is computed to be 1000 bits with a link quality of BER = 0.0001 (or 10^{-4}) using a packet header of 80 bits, then E_{2M} is found to be 0.83 in Figure 5.2. It is essential to mention here that there are several other graphs and also their corresponding databases as shown in Appendix F (some samples) similar to Figure 5.2 which can be plotted under different header length. All these graphs/databases would be used to determine the various E_{2M} values for filling up the E_{2M} column in Table 5.6.

Lastly, the columns E_{2Q} and N_{2Q} clearly are, the energy efficiency and the relevant optimal packet size computed from the proposed 2Q algorithm. All values entered into the columns N_{2M}, E_{2M}, E_{2Q}, and N_{2Q} would then be used to plot graphs for analysis and comparative study purposes.

It is apparent from the format of Table 5.6 that there are ample possibilities in grouping the header length values and the *lR*-product values under one table. It is so because there are eight different header length values in Figure 5.1 and ten *lR*-product values in Figure 5.6. To avoid making this dissertation into volumes by including tables for all the possibilities, the author have chosen only three header length of 30 bits, 60 bits, and 100 bits from Figure 5.1. It is done in this way because these headers are adequate to cover the header size ranging from 30 bits to 100 bits.

For the *lR*-product, two values of 1×10^5 m-bps (i.e.10-meter range with 10 kbps data rate) and 9×10^5 m-bps (90-meter ramge with 10 kbps data rate) were chosen from graphs similar to Figure 5.2. It should be pointed out that the *lR*-product values were chosen to represent a near field transmission and also a far field transmission. The header length and the *lR*-product values were chosen based on the practical parameters commonly used in general non-military UWA data transmission. Full table entries for Table 5.6 can be found in Appendix P.

By referring to the full information from Table 5.7 in Appendix P, six graphs were plotted for comparisons. These graphs are shown in Figure 5.10 to Figure 5.15. The values of the header length and the *lR*-product used in each plot are stated in the caption of each graph respectively.

Take note that each of these graphs comprises of four curves representing N_{2M}, E_{2M}, E_{2Q}, and N_{2Q}. It can be seen clearly in Figure 5.10 to Figure 5.15 that N_{2M} can be explicitly compared to N_{2Q}, and E_{2M} explicitly to E_{2Q}. Also, N_{2M} with its E_{2M} can be explicitly compared to N_{2Q} with its E_{2Q}.

For a near field transmission (Figure 5.10 to 5.12) it is evident that the energy efficiency (E_{2M} and E_{2Q}) for 2M approach and the proposed 2Q algorithm is comparable to each other. However, in terms of optimal packet size, it seems that N_{2M} is always better than N_{2Q}.

Based on the information tabulated in Table 5.6 (Appendix P), the author's analysis on the near field transmission shows that the best case difference between E_{2Q} and E_{2M} is found to be around 3.8%, and on the average, N_{2M} is better than N_{2Q} by about 23%.

This analysis suggests that the proposed 2Q algorithm slightly outperforms the 2M approach in the context of energy efficiency but lost out in terms of optimal data packet size. In other words, for near field transmission, it is sufficient to have two performance metrics to qualify an optimal packet size for data transmission.

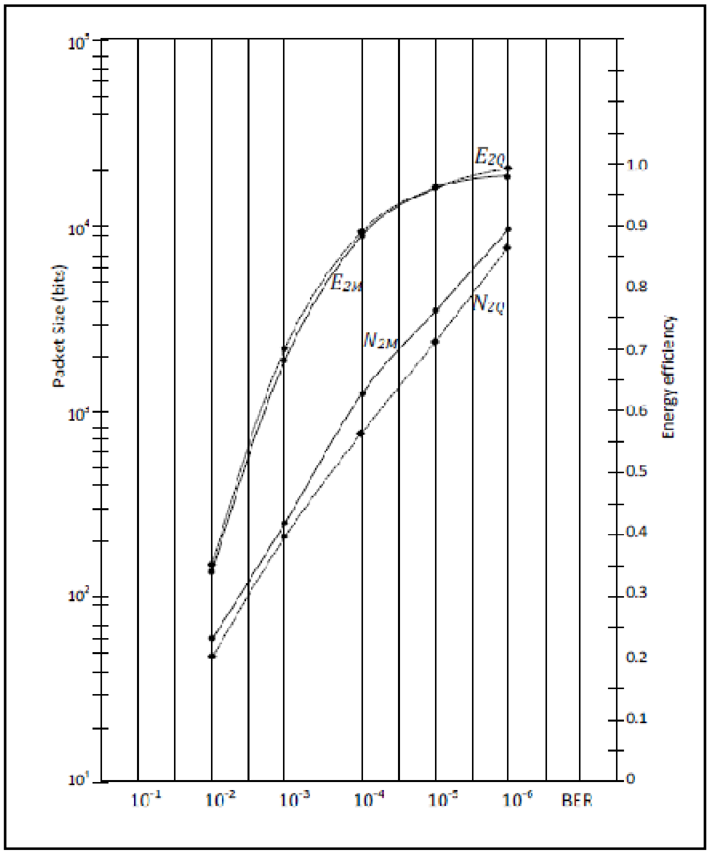

Figure 5.10: Comparison of optimal packet size and energy efficiency between 2M and 2Q approaches based on the data tabulated in Appendix P with header length of 30 bits and IR product of $1x10^5$ m-bps.

These findings, in fact, can be explained in the sense that for a near filed transmission the chances/probabilities for a data packet to be corrupted are statistically less and it is possible to transmit a larger packet size [17].

Furthermore, with less chances of packet corruption, it follows that the request for packet retransmission is consequently reduced. Meaning that less energy would be wasted (or used) for retransmission processes. It is reasonable then to transmit data packet of larger sizes and at the same time to maintain a good energy efficiency.

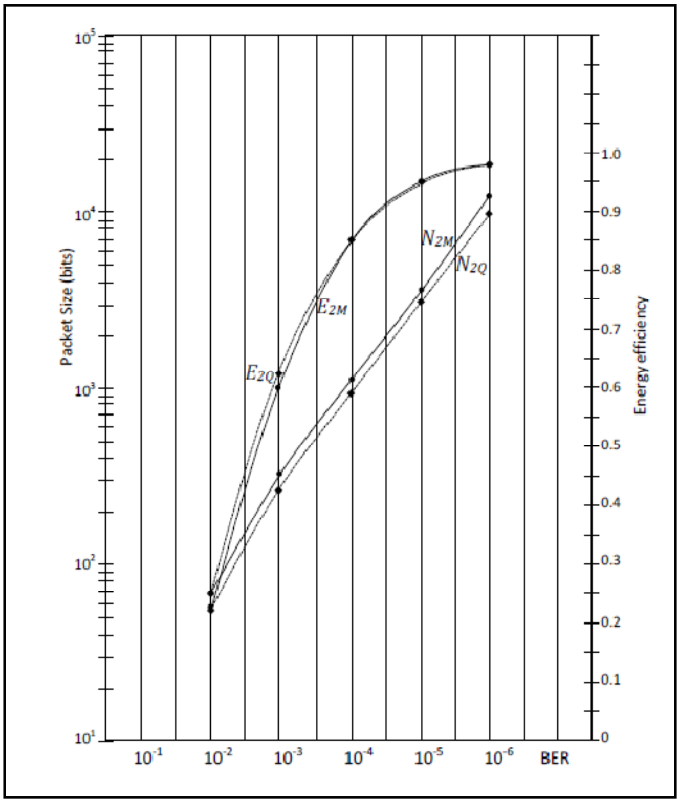

Figure 5.11: Comparison of optimal packet size and energy efficiency between 2M and 2Q approaches based on the data tabulated in Appendix P with header length of 60 bits and *IR* product of 1x10^5 m-bps.

Some general observations in Figure 5.10 to 5.15 reveal that:

(i) As the quality of the link improves, the optimal data packet size grows quite linearly with it. This is acceptable since data bits suffer less corruption in a quality link causing that more bits are allowed to be packed into a packet.

(ii) High energy efficiency, of more than 90%, is attained when the link quality is having a BER of more than 10^{-5}, regardless of near field or far field transmission. This shows that a quality link can support a more reliable data bits transmission, and to a certain extent, helps to reduce energy wastage.

(iii) Energy efficiency could be an important issue/factor in field deployment if the quality (BER) of the link is found between the ranges of 10^{-2} to 10^{-5}. Within this range the energy efficiency can vary from as low as 30% to about 80%.

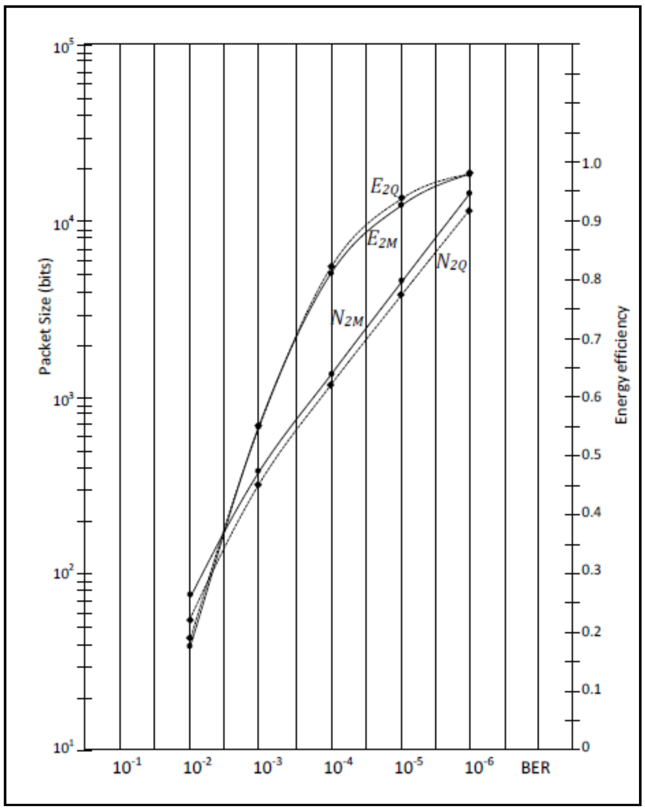

Figure 5.12: Comparison of optimal packet size and energy efficiency between 2M and 2Q approaches based on the data tabulated in Appendix P with header length of 100 bits and *lR* product of $1x10^5$ m-bps.

It is necessary to inform that all the graphs plotted in Figure 5.10 to 5.15 do not take BER of 10^{-1} into consideration. The reason is straightforward because in practical data transmission this value of BER denotes a very low link quality which is not worth for transmitting data packets meaningfully. Demand for data packet retransmission at BER of 10^{-1} would be generally high and thus high energy wastage goes with it.

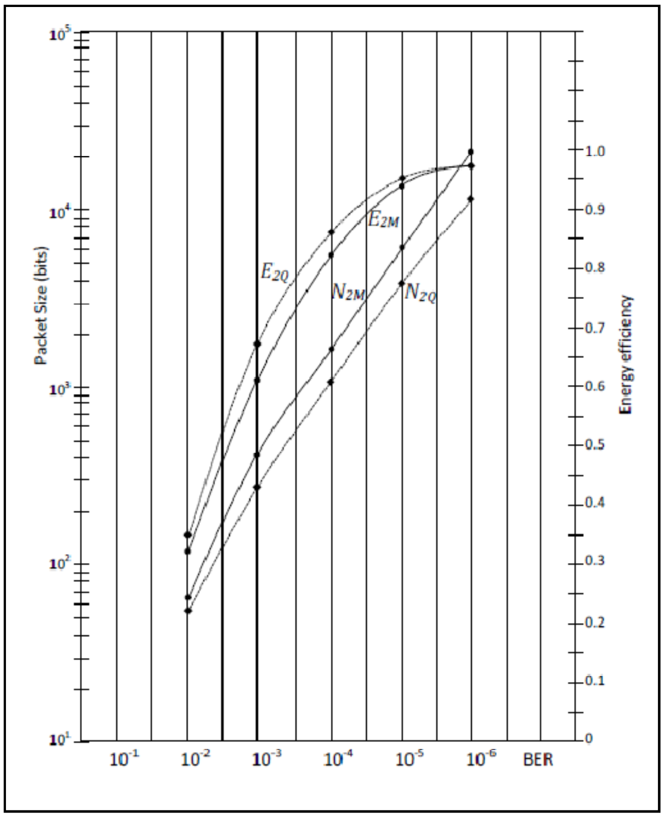

Figure 5.13: Comparison of optimal packet size and energy efficiency between 2M and 2Q approaches based on the data tabulated in Appendix P with header length of 30 bits and *lR* product of 9×10^5 m-bps.

For far field transmission, the readers are to refer to Figure 5.13 to 5.15 for seeing the comparisons between the 2M and the 2Q algorithms. It can be seen that the E_{2Q} of the proposed 2Q algorithm seems to perform much better than E_{2M}. That is, E_{2M} is no more comparable to E_{2Q} as in the case of near field transmission.

Again, with reference to the information tabulated in Appendix P for far field data transmission, the author's analysis showed that on the average, E_{2Q} outperforms E_{2M} by about 38%. Then, in terms of packet size, it is clearly manifested in Figure 5.13 to 5.15 that N_{2M} is always larger than N_{2Q}.

In fact, from the author's analysis based on the data in Appendix P, it can be shown that N_{2M} on average is larger than N_{2Q} by 41%. This finding amount to the fact that for a longer transmission range the probability for data packet getting corrupted is naturally higher [17] in view of harsh underwater environment (in fact is similar in terrestrial radio wave transmission environment too). For this, the demand for data packet re-transmission is certainly to be more frequent making energy efficiency to suffer i.e. larger packet size that comes with lower energy efficiency.

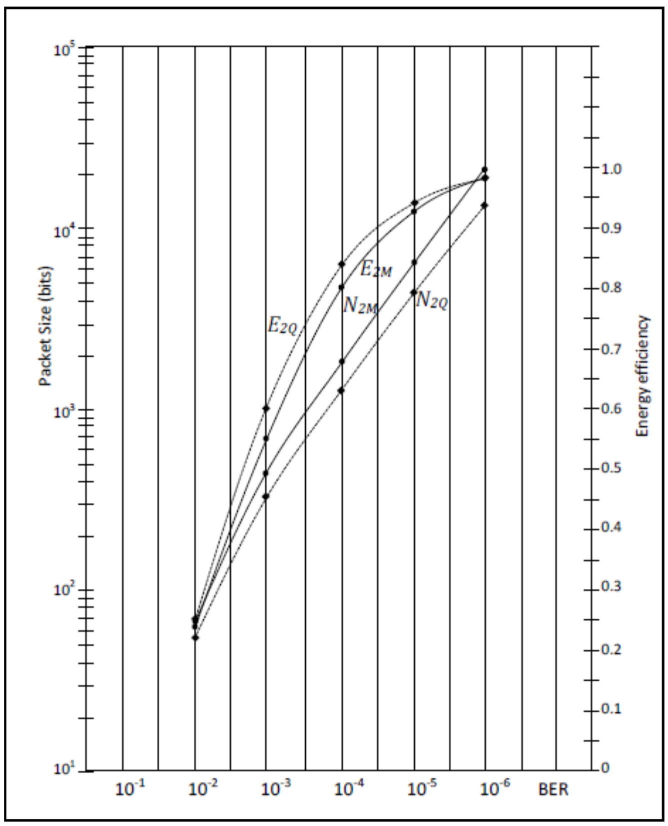

Figure 5.14: Comparison of optimal packet size and energy efficiency between 2M and 2Q approaches based on the data in Appendix P with header length of 60 bits and *lR*-product of $9x10^5$ m-bps.

These analyses bring out a point of concern in far field transmission for optimal data packet size computation. There could be a compromise between the 2M approach and the proposed 2Q approach. In 2M approach, a larger packet size can be used but with lower energy efficiency. On the other hand, in 2Q approach, a smaller packet size is transmitted with an advantage to gain on higher energy efficiency.

Practically it is suggested that if energy conservation is not an issue in the sensor node (such as powered by a rechargeable/replaceable power source), then 2M approach is a better choice than 2Q. Conversely, 2Q approach should be a priority over the 2M approach.

The reader should notice that in Figure 5.13 to Figure 5.15 the energy efficiency advantage of E_{2Q} over the E_{2M} is more noticeable within the BER range of 10^{-3} to 10^{-5}. When the link quality is not good (BER at 10^{-2} and below), and when it is good (10^{-5} and above), E_{2M} and E_{2Q} are found to be comparable to each other, indicating that there is no significant advantage of E_{2Q} over E_{2M}.

These phenomena could be explained from the fact that at bad BER, regardless of the packet size i.e. it does not matter if N_{2M} is larger than N_{2Q} (or vice versa), the data bits in the packet can always be easily corrupted. Therefore there is always a high frequency for packet retransmissions causing the energy efficiency to be generally low. At the other end when BER is good, the data bits in the packet are always delivered with high integrity regardless of the packet size. In this situation the frequency for retransmissions is generally low, consequently making data packet transmissions to be highly effective and generally able to be attained for high energy efficiency.

The author would like to point out at this juncture that the practical underwater data communication link quality is normally specified within the BER's range of 10^{-3} to 10^{-5}. For instance, in a practical QPSK (Quadrature Phase-Shift Keying) system using a data rate of 5kbps with a carrier frequency of 15 kHz, the BER is about 10^{-3}. In fact the author's research work was focused to propose an algorithm targeted for implementation in a practical UWA channel for tropical shallow water environment.

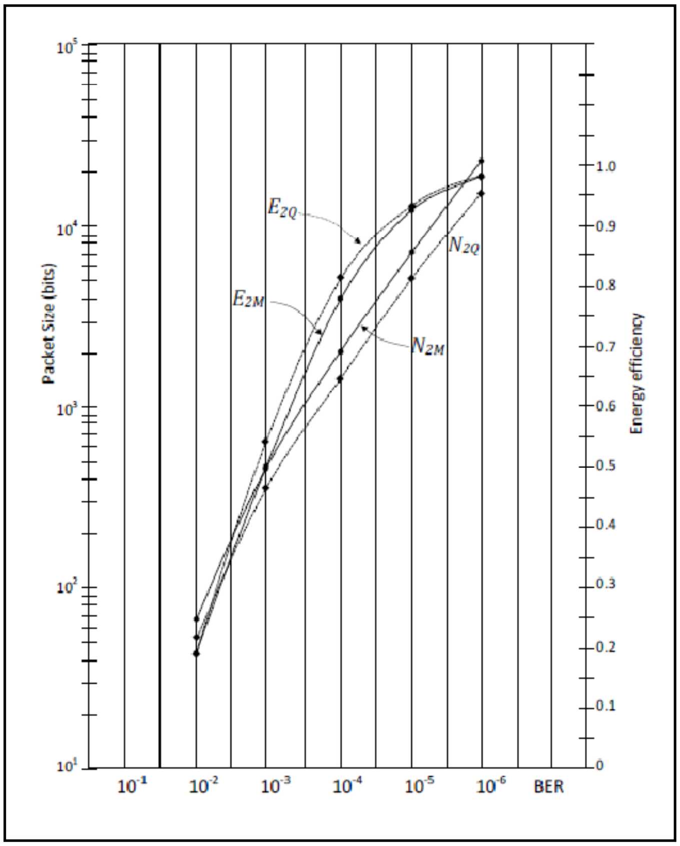

Figure 5.15: Comparison of optimal packet size and energy efficiency between 2M and 2Q approaches based on the data in Appendix P with header length of 100 bits and *lR* product of $9x10^5$ m-bps.

5.3 Chapter Conclusions

The detailed analysis and comparative studies in this chapter in fact are the extension of the simulation works accomplished in chapter 4. Strong references were made to the results and data collected from the simulations in the previous chapter. A large amount of relevant data were generated and collected from those simulations from which various data sets and tables can be constructed to plot various graphs to do the various intended analyses and comparative studies.

It should be clarified here that these studies are not a form of benchmarking against any known data packet size optimization algorithm or technique, but are to find out how the proposed 2Q algorithm may performs in comparison to algorithm using single metric and algorithm using dual metrics (2M). The outcomes of the analyses and comparative studies shall allow the author to better understand the performance of the proposed algorithm and to see whether the main objective of this research work is met.

Three comparative studies were discussed in details by focusing on optimal data packet size based on BER alone, qualified by throughput efficiency alone, and based on combination of BER and throughput efficiency. All these studies were in the context of energy efficiency because energy conservation is considered one of the main issues in underwater acoustic communications where majority of the sensor nodes are powered by a power source that is not rechargeable or replaceable.

The outcomes of the first comparative studies show that the proposed algorithm outperforms the approach in using BER as a single metric in terms of larger packet size with comparable energy efficiency. In the second comparative studies the proposed algorithm was compared to the approach using throughput efficiency as the single qualifier, where the author found that the proposed algorithm was able to compute a data packet size with higher energy efficacy than the packet size computed based on throughput efficiency alone. Then in comparing the proposed 2Q algorithm to the dual metrics (2M) approach, there are two cases of interest, namely the near field transmission and the far field transmission cases.

For near field transmission the proposed 2Q algorithm shows comparable energy efficiency to the 2M approach but suffers a little in terms of packet size. For the far field transmission the proposed 2Q algorithm is much better than the 2M approach in terms of energy efficiency but suffers a higher disadvantage in terms of packet sizes.